ANNALES
UNIVERSITATIS MARIAE CURIE-SKŁODOWSKA
LUBLIN — POLONIA
VOL. XLVIII, 15 SECTIO AAA 1993

Institute of Physics, Maria Curie-Skłodowska University

Lucjan E. MISIAK[a], Wiesława KORCZAK[a,b], Sushil K. MISRA[c] and Piotr MAZUREK[a]

A Study of Low-Level Doped High-T_c Superconductors $Y_{1-x}R_xBa_{2-y}Me_yCu_3O_{7-\delta}$ (R = Gd, Me = Sr) and $YBa_2M_xCu_{3-x}O_{7-\delta}$ (M = Cr, Ni, Fe, Mn)

Badania niskodomieszkowych wysokotemperaturowych nadprzewodników typu $Y_{1-x}R_xBa_{2-y}Me_yCu_3O_{7-\delta}$ (R = Gd, Me = Sr) i $YBa_2M_xCu_{3-x}O_{7-\delta}$ (M = Cr, Ni, Fe, Mn)

1. INTRODUCTION

The influence of atomic substitution at different crystallographic positions in a high-T_c superconductor is an important tool for probing the parameters characterizing its superconductivity. Doping with different ions of the high-T_c superconductor $YBa_2Cu_{3-x}O_{7-\delta}$, influences the superconducting properties; the effect is particularly significant when the substitution is at the Cu-positions [1–5].

The series of doped ceramics $YBa_2M_xCu_{3-x}O_{7-\delta}$ (M= Fe, Cr, Mn, Ni, Co, Zn) have been studied by a variety of experimental techniques, e.g. resistance [6, 7, 8], Mössbauer [9, 10, 11], ac-magnetic susceptibility [12, 13, 14], SQUID [15], neutron and X-ray diffraction [16, 17], specific heat [18], thermoelectric power [19], and transmission electron microscopy [20]. The superconducting properties depend upon the amount of doping, and the kind of Cu sites — Cu(1) or Cu(2) — substituted by the doping ions. The dopants perturb the electronic structure of the Cu and O ions, whose

[a] Experimental Physics Department, Maria Curie-Skłodowska University, Plac M. Curie-Skłodowskiej 1, 20–031 Lublin, Poland.

[b] Centre de Recherches sur les Très Basses Températures, CNRS, 166X–38042 Grenoble Cedex, France.

[c] Department of Physics, Concordia University, 1455 de Maisonneuve Boulevard West, Montréal, Québec, Canada H3G 1M8.

spd hybridization states provide the superconducting electrons. The Ni ions preferably occupy the Cu(2) sites, whereas the Fe ions occupy both the Cu(1) and Cu(2) sites [21], although preferably Cu(1). Liang et al. [22] showed that substitution of Cu in $YBa_2Cu_3O_{7-\delta}$ by small amounts of Ni and Zn did not significantly alter the oxygen content. X-ray studies of these compounds confirmed the existence of the orthorhombic structure, and δ was found to be below 0.1 [14, 23].

This paper reports a detailed study based on the measurements of resistivity, ac-susceptibility and low-field microwave absorption on $YBa_2Cu_3O_{7-\delta}$ (YBaCuO, hereafter) samples doped with Sr, Gd, Cr, Mn, Fe, Ni ions in order to study the influence of small level of doping, and the effect of different ions on superconducting properties of YBaCuO. The previously-studied samples were doped with a rather high concentration (0.3–10%) of 3d elements. In contrast, in the present paper, the lowest concentration of doping with Fe (0.003%) is 1/100th that (0.3%) used by Moorjani et al. [10], and 1/3000th that used (10%) for Cr, Mn, Fe, and Ni by Xiao et al. [14].

2. SAMPLE PREPARATION, STRUCTURE AND EXPERIMENTAL ARRANGEMENT

Samples were prepared from powders consisting of nominal amounts of Y_2O_3, $BaCO_3$, CuO, and the specific compounds required to substitute for Cu, Y or Ba (Ni_2O_3, Cr_2O_3, Fe, $MnCl_2{\cdot}H_2O$, Gd_2O_3, $SrCO_2$). The same conditions were used in the preparation of all the samples for purposes of comparison, and in order to maintain the oxygen content at the same level. In each case, a mixture of adequate proportions of respective powders, mixed thoroughly in methyl alcohol, was ground. The powders were thereafter heated at 910° C for 12 hours in air atmosphere. Mixing and grinding were repeated a few times. Thereafter, the resulting products were pressed into pellets and sintered at 945°C for 12 hours in an atmosphere of flowing oxygen gas. The pellets were finally brought to room temperature with a cooling rate of 20°C/h. The structures of all the samples were found to be orthorhombic from the respective powder X-ray diffraction patterns recorded on a Dresden VEB HZG-4 diffractometer. The lattice constants of the various doped samples were found to be only slightly different from those of the pure $YBa_2Cu_3O_{7-\delta}$ ceramic: $a = 0.382$, $b = 0.389$, $c = 1.169$ nm.

Resistivity measurements were carried out on samples cut to appropriate sizes from pellets. The standard four-probe method, using a current density in the range of 0.01–0.1 A/cm^2, in conjunction with computer acquisition of data was used to record ac-electrical resistivity. The real and imaginary

parts of the complex ac-susceptibility ($\chi_{AC} = \chi' - i\chi''$) were measured with a mutual inductance bridge operating at a low frequency (110 Hz) and at low magnetic fields (< 0.4 mT).

Low-field microwave absorptions were measured on an X-band EPR spectrometer, equipped with Helmholtz coils in order to provide small reverse magnetic fields.

3. EXPERIMENTAL RESULTS AND DISCUSSION

A. **ac-electrical resistivity.** The data reveal the two-steps character of decrease of resistivity with lowering temperature for the various doped samples (Fig. 1). It is seen from Table 1 that the substitution of Cu even by very small amounts of Mn, Fe, Cr, and Ni resulted in a significant decrease of $T_c^{R=0}$ from that for a pure sample. The 3d dopants lower $T_c^{R=0}$ by (i) producing local disorder and trapping the electrons responsible for superconductivity, thus partially suppressing superconductivity, (ii) breaking of pairs by conduction and exchange scattering of 3d-electrons at a paramagnetic site [14, 24], (iii) conventional spin-exchange [8], (iv) loss of oxygen after doping of sample [8], and (v) filling of holes in the oxygen valence band [8].

A large amount of Sr (25%) doped for Ba in $Y_{0.99}Gd_{0.01}Ba_{1.5}Sr_{0.5}Cu_3O_{7-\delta}$ lowered $T_c^{R=0}$ to 70.5 K, similar to that observed by Sung et al. [25]. The resistivity behaviour of the sample doped with Gd for Y was found to be the same as that of the pure $YBa_2Cu_3O_{7-\delta}$. This is because superconductivity occurs in copper-oxygen planes influenced by oxygen vacancies, while the Y and Ba atoms only provide structural stabilization.

B. **ac-complex susceptibility.** The values of the real (χ') and imaginary (χ'') parts of the ac-complex susceptibility as measured for the samples $YBa_2Cu_3O_{7-\delta}$, $YBa_2Mn_{0.01}Cu_{2.99}O_{7-\delta}$, and $YBa_2Mn_{0.005}Cu_{2.995}O_{7-\delta}$ at various temperatures are depicted in Figure 2. It is seen that both χ' and χ'' exhibit two-steps decreases in their values with decreasing temperature. The first step indicates the onset of superconductivity and the second represents the low-temperature anomaly, i.e. an unexpected increase in the real part of susceptibility (χ') and the appearance of a hump in the imaginary part of the susceptibility (χ'') (indicated by arrows in Fig. 2). The low-temperature anomaly is caused by muliticonnected Josephson networks among the superconducting grains, and appears only in bulk samples for ac-magnetic fields greater than 0.5 mT [13]. At temperatures below 60 K, periodic oscillations were observed in the values of χ' for the undoped sample (Fig. 2) measured in an ac-magnetic field of amplitude 0.0008 mT.

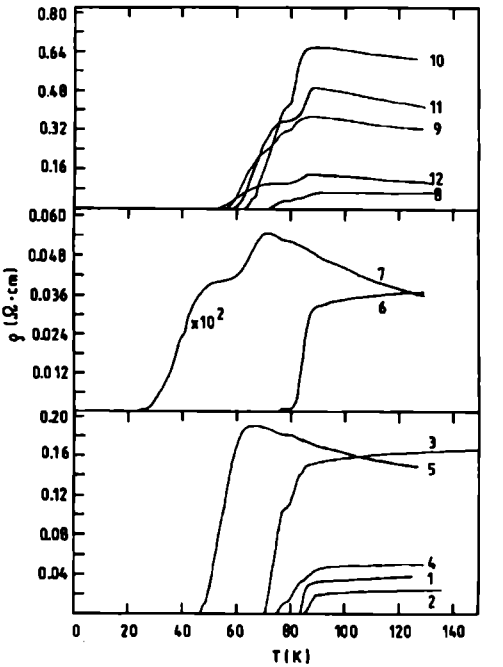

Fig. 1. A plot of the resistance versus temperature for the various investigated samples. The samples are numbered as follows: (1) $YBa_2Cu_3O_{7-\delta}$ (2) $Y_{0.99}Gd_{0.01}Ba_2Cu_3O_{7-\delta}$ (3) $Y_{0.99}Gd_{0.01}Ba_{1.5}Sr_{0.5}Cu_3O_{7-\delta}$ (4) $YBa_2Cr_{0.005}Cu_{2.995}O_{7-\delta}$ (5) $YBa_2Cr_{0.05}Cu_{2.95}O_{7-\delta}$ (6) $YBa_2Ni_{0.005}Cu_{2.995}O_{7-\delta}$ (7) $YBa_2Ni_{0.05}Cu_{2.95}O_{7-\delta}$ (8) $YBa_2Fe_{0.001}Cu_{2.999}O_{7-\delta}$ (9) $YBa_2Fe_{0.01}Cu_{2.99}O_{7-\delta}$ (10) $YBa_2Mn_{0.001}Cu_{2.999}O_{7-\delta}$ (11) $YBa_2Mn_{0.005}Cu_{2.995}O_{7-\delta}$ (12) $YBa_2Mn_{0.01}Cu_{2.99}O_{7-\delta}$

Ryc. 1. Wykres zależności oporu od temperatury dla badanych próbek. Próbki są numerowane następująco: (1) $YBa_2Cu_3O_{7-\delta}$ (2) $Y_{0.99}Gd_{0.01}Ba_2Cu_3O_{7-\delta}$ (3) $Y_{0.99}Gd_{0.01}Ba_{1.5}Sr_{0.5}Cu_3O_{7-\delta}$ (4) $YBa_2Cr_{0.005}Cu_{2.995}O_{7-\delta}$ (5) $YBa_2Cr_{0.05}Cu_{2.95}O_{7-\delta}$ (6) $YBa_2Ni_{0.005}Cu_{2.995}O_{7-\delta}$ (7) $YBa_2Ni_{0.05}Cu_{2.95}O_{7-\delta}$ (8) $YBa_2Fe_{0.001}Cu_{2.999}O_{7-\delta}$ (9) $YBa_2Fe_{0.01}Cu_{2.99}O_{7-\delta}$ (10) $YBa_2Mn_{0.001}Cu_{2.999}O_{7-\delta}$ (11) $YBa_2Mn_{0.005}Cu_{2.995}O_{7-\delta}$ (12) $YBa_2Mn_{0.01}Cu_{2.99}O_{7-\delta}$

C. **Microwave absorption.** The microwave absorption is caused by the damped motions of fluxons driven by induced microwave supercurrents, with the largest contribution coming from the fluxons situated in the weakest Josephson junctions [26].

Zero-field cooling. The $YBa_2Mn_{0.001}Cu_{2.999}O_{7-\delta}$ sample (Fig. 3a) exhibited N-shaped line in the microwave absorption (zero-field cooling) for magnetic field sweep from −5 to +5 mT at temperatures between 24 and 50 K. A characteristic feature of the spectra was the hysteresis in the microwave absorption that existed between magnetic field sweeps in

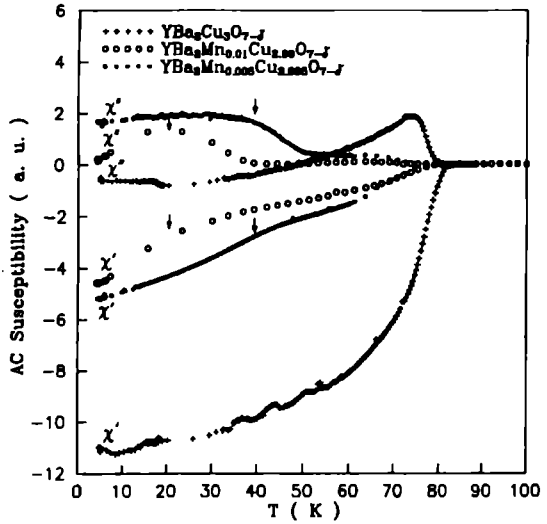

Fig. 2. Temperature dependencies of the real (χ') and imaginary (χ'') parts of the complex ac-susceptibility in arbitrary units (a.u.), measured using an ac-magnetic field of amplitude 0.0008 mT and of frequency 110 Hz. The arrows indicate the anomalies exhibited by χ' and χ'' at low temperatures

Ryc. 2. Zależność od temperatury części rzeczywistej (χ') i urojonej (χ'') zespolonej zmiennoprądowej podatności magnetycznej w jednostkach względnych (a.u.), mierzonej z użyciem zmiennego pola magnetycznego o amplitudzie 0,0008 mT i częstotliwości 110 Hz. Strzałki wskazują anomalie wykazywane przez χ' i χ'' w niskich temperaturach

the forward and reverse directions. The hysteresis of microwave absorption was enhanced when the temperature is raised close to the superconducting transition temperature as observed presently for $YBa_2Mn_{0.001}Cu_{2.999}O_{7-\delta}$ and $YBa_2Ni_{0.005}Cu_{2.995}O_{7-\delta}$ (Figs. 3a, b). This is due to the creation of critical state when the external magnetic field has entered part of the superconducting sample, as well as due to the pinning and depinning of the fluxons during a cycle of the modulation field [27]. On the other hand, there is also hysteresis due to trapped flux if the direct absorption is measured without using the modulation technique. The hysteresis area is almost completely suppressed to zero for the Mn-doped sample.

Field cooling. The samples were also cooled under the action of a magnetic field, which was turned off when the desired temperature was reached. The microwave absorption (field cooling) depended on the strength of the magnetic field to which the sample was exposed during cooling, and the interval of time that elapsed before the microwave absorption was recorded. The higher was the magnetic field intensity during cooling the

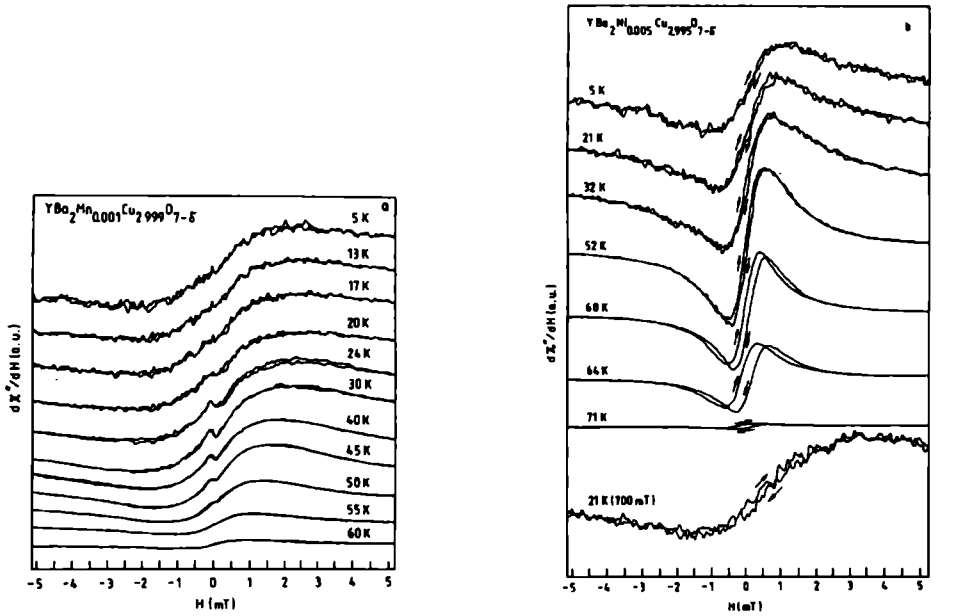

Fig. 3. Low-field microwave absorption in arbitrary units (a. u.) measured at different temperatures in the samples (a) $YBa_2Mn_{0.001}Cu_{2.999}O_{7-\delta}$ and (b) $YBa_2Ni_{0.005}Cu_{2.995}O_{7-\delta}$. Note the difference in the spectra at 21 K (b) measured after zero magnetic field cooling and that measured after exposure of the sample to 700 mT magnetic field (the lowest spectrum). The spectra were recorded for forward and reverse directions of the external magnetic field as indicated by the arrows

Ryc. 3. Niskopolowa absorpcja mikrofalowa w jednostkach względnych (a.u.) zmierzona w różnych temperaturach w próbkach (a) $YBa_2Mn_{0.001}Cu_{2.999}O_{7-\delta}$ i (b) $YBa_2Ni_{0.005}Cu_{2.995}O_{7-\delta}$. Należy odnotować różnicę w widmie w 21 K (b) zmierzonym po schłodzeniu próbki w zerowym polu magnetycznym, a zmierzonym po umieszczeniu próbki w 700 mT polu magnetycznym (najniższe widmo). Widma były rejestrowane w kierunku wzrostu zewnętrznego pola magnetycznego i przeciwnym, zgodnie ze strzałkami

bigger was found the shift in the positions of the maxima of microwave absorption. The difference between shifts in the positions of the maxima 0.9 and 3.5 mT, observed after cooling in zero and in 0.7 T external magnetic fields, respectively, at 21 K for the sample $YBa_2Ni_{0.005}Cu_{2.995}O_{7-\delta}$ (Fig. 3b) is quite significant. This difference in the shifts arises due to trapped fluxons (frozen magnetic field) in heterogeneous materials.

Microwave absorption under exposure to 100 kHz modulation. Figure 4 shows the low-field microwave absorption at 79.5 K as a function of magnetic field intensity for Cr-doped sample exposed to 100 kHz modulation of various amplitudes. The amplitude of the 100 kHz modulation (H_m) influenced the position of the maximum of microwave absorption only when it was greater than a certain peak-to-peak value, equal to twice the

lower-critical field $2H_{c1}^*$ ($=\sim 0.5$ mT for $YBa_2Ni_{0.005}Cu_{2.995}O_{7-\delta}$) being the field separation between the forward and reverse critical states. When the amplitude of the modulation field is sufficiently large, fluxons are swept out of the sample.

D. **Thermodynamic (H_c^*)/upper critical (H_{c2}^*) fields and Sommerfeld constant** (γ). The lower critical field (H_{c1}^*) is defined by the position of the maximum of microwave absorption for forward direction of the external magnetic field under zero field cooling conditions. The thermodynamic (H_c^*) and the upper (H_{c2}^*) critical fields, as well as the Sommerfeld constant (γ-known as the coefficient of the normal electronic specific heat

Table 1. The values of the parameters characterizing the various samples, where $T_c^{R=0}$ is the transition temperature at which the resistance of the sample becomes zero (the underlined values of $T_c^{R=0}$ are related to onset of superconductivity), $H_{c1}^*(0)$, $H_c^*(0)$, and $H_{c2}^*(0)$ are lower, thermodynamic, and upper critical fields extrapolated to 0 K, respectively, and γ is the Sommerfeld constant

Tab. 1. Wartości parametrów charakteryzujących poszczególne próbki; $T_c^{R=0}$ jest temperaturą przejścia, przy której $R = 0$ (podkreślone wartości $T_c^{R=0}$ dotyczą pojawienia się nadprzewodnictwa; $H_{c1}^*(0)$, $H_c^*(0)$, i $H_{c2}^*(0)$ są polami krytycznymi odpowiednio: niższym, termodynamicznym, wyższym, ekstrapolowanymi do 0 K, a γ jest stałą Sommerfelda

Sample Sample	$T_c^{R=0}$ (K)	$H_{c1}^*(0)$ (mT)	$H_c^*(0)$ (mT)	$H_{c2}^*(0)$ (T)	γ (μJ/cm^{3}K^2)
$YBa_2Cu_3O_{7-\delta}$	83.5				
$Y_{0.99}Gd_{0.01}Ba_2Cu_3O_{7-\delta}$	85	1.39	74	21	0.6
$Y_{0.99}Gd_{0.01}Ba_{1.5}Sr_{0.5}Cu_3O_{7-\delta}$	**73**				
	70.5				
$YBa_2Cr_{0.005}Cu_{2.995}O_{7-\delta}$	**78**				
	74.5	1.08	58	16	0.5
$YBa_2Cr_{0.05}Cu_{2.95}O_{7-\delta}$	**47**				
$YBa_2Ni_{0.005}Cu_{2.995}O_{7-\delta}$	**82**				
	75	1.25	67	19	0.6
$YBa_2Ni_{0.005}Cu_{2.95}O_{7-\delta}$	**47**				
	24				
$YBa_2Fe_{0.001}Cu_{2.999}O_{7-\delta}$	**80**				
	76				
	71				
$YBa_2Fe_{0.01}Cu_{2.99}O_{7-\delta}$	**68**				
	64				
	56.5				
$YBa_2Mn_{0.001}Cu_{2.999}O_{7-\delta}$	**73**				
	63	2.70	144	41	4.2
$YBa_2Mn_{0.005}Cu_{2.995}O_{7-\delta}$	**71**				
	59				
$YBa_2Mn_{0.01}Cu_{2.99}O_{7-\delta}$	**67**				
	52				

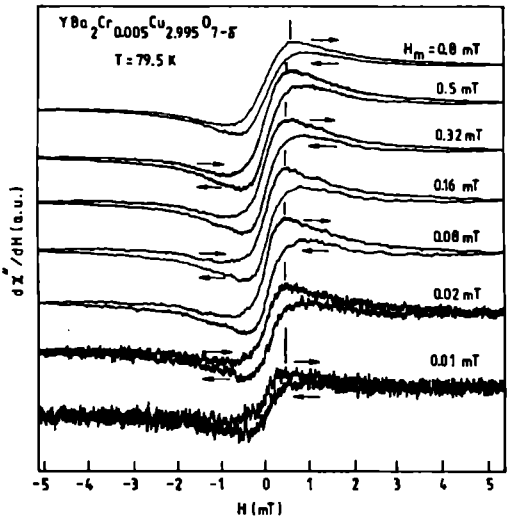

Fig. 4. Low-field microwave absorption in arbitrary units (a.u.) of $YBa_2Cr_{0.005}Cu_{2.995}O_{7-\delta}$, recorded for forward and reverse directions of $\vec{B}$ using various 100 kHz modulation field amplitudes (H_m). Every vertical dash shows the position of microwave absorption peak

Ryc. 4. Niskopolowa absorpcja mikrofalowa w jednostkach względnych (a.u.) w $YBa_2Cr_{0.005}Cu_{2.995}O_{7-\delta}$ zarejestrowana w kierunku wzrostu $\vec{B}$ i przeciwnym z użyciem różnych amplitud modulacji pola magnetycznego o częstości 100 kHz (H_m). Każda pionowa kreska pokazuje położenie wierzchołka absorpcji mikrofalowej

$C_{en} = \gamma T$) were calculated from the relations given in [3, 29]. The γ can be also determined from the relation $\gamma = 2/3\pi^2 k_B^2 N(0)$, where $N(0)$ is the bare density of states of the Fermi surface at 0 K and k_B is the Boltzmann constant.

The required value of $\kappa(\equiv \lambda/\xi)$ used was 200 (penetration depth (λ) = 220 nm, coherence length (ξ) = 1.1 nm [30]), lying in the range of κ values 100–200 for $YBa_2Cu_3O_{7-\delta}$ [30–32]. The estimated values of $H_c^*(0)$, $H_{c2}^*(0)$ and γ for the samples doped with Gd, Cr, Ni, and Mn are listed in Table 1. These values of $H_{c2}^*(0)$ are less (20–50%) than those reported for the pure YBaCuO sample which are in the range 80–148 T [33, 34].

E. **Linewidth broadening of DPPH below $T_c^{R=0}$.** The penetration depth (λ_0) as determined from the EPR line of a thin layer of DPPH deposited on the surface of $YBa_2Ni_{0.005}Cu_{2.995}O_{7-\delta}$ was studied as a function of temperature. The peak-to-peak first derivative linewidth (ΔH_{pp}) and the amplitude (I) of adsorbed DPPH after the sample became superconducting were found to exhibit drastic changes as functions of temperature (Fig. 5). (There was observed an overlap of DPPH line by another line just below

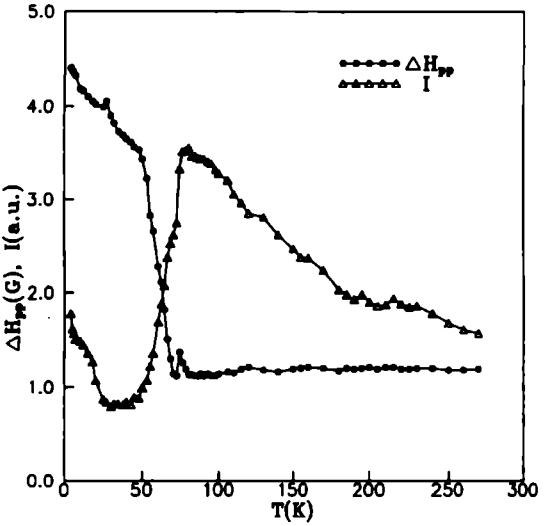

Fig. 5. Temperature dependence of the peak-to-peak linewidth (ΔH_{pp}) and the peak-to-peak intensity (I) in arbitrary units (a.u.) of the first-derivative absorption signal of a thin layer of DPPH adsorbed on the surface of the sample $YBa_2Ni_{0.005}Cu_{2.995}O_{7-\delta}$
Рис. 5. Залежність від температури ширини лінії I зміряних від вершини до вершини (ΔH_{pp}) і інтенсивності лінії (I) зміряної від вершини до вершини в одиницях (a.u.) першої похідної сигналу абсорбції тонкого шару DPPH адсорбованого на поверхні зразка $YBa_2Ni_{0.005}Cu_{2.995}O_{7-\delta}$

$T_c^{R=0}$; this line moved to higher magnetic fields with lowering temperature.) When the sample becomes superconducting, the penetration of magnetic field, in the form of Abrikosov vortices changes, causing a broadening of the DPPH line, whose width is described by the following expression [35, 36]:

$$\Delta H_{pp} = 2\left[\overline{\Delta H_n^2} + \overline{\Delta H_s^2}\right]^{1/2}, \tag{1}$$

where $\overline{\Delta H_s^2} = \frac{\phi_0^2}{16\pi^3\lambda^4}$, is the second moment of the field distribution, $\lambda = \lambda_0/[1-(T/T_c)^4]$, λ_0 is the penetration depth extrapolated to zero temperature, $\phi_0 = 2.07 \times 10^{-15}\ m^2T$, and $\overline{\Delta H_n^2}$ is the second moment of the EPR line in the normal state at temperatures just above $T_c^{R=0}$. Finally,

$$\Delta H_{pp} = \left\{\overline{\Delta H_{pp(n)}^2} + \frac{\phi_0^2}{4\pi^3\lambda_0^4}\left[1-\left(\frac{T}{Tc}\right)^4\right]^2\right\}^{1/2}, \tag{2}$$

where $\overline{\Delta H_{pp(n)}}[= 2(\overline{\Delta H_n}^2)^{1/2}]$ is the peak-to-peak linewidth in the normal state at temperatures just above $T_c^{R=0}$.

The values of λ_0 and $T_c^{R=0}$ were presently estimated to be 690 nm and 75 K fitting ΔH_{pp} to T using eq. (2). This value of λ_0 for the sample which contains a very small amount of Ni ions, is much larger than those reported in the literature for the pure $YBa_2Cu_3O_{7-\delta}$ (140–250 nm) [37, 38].

4. CONCLUDING REMARKS

The effect of doping of the YBaCuO ceramic with the elements Gd, Sr, Cr, Mn, Fe, Ni on its superconducting properties as found from the present studies can be summarized as follows:

(i) Even very small concentrations of the 3d-group dopants Cr, Mn, Fe, and Ni significantly lower $T_c^{R=0}$ by partially destroying antiferromagnetic couplings and resonance of bindings in CuO_2 chains. On the other hand, doping with a rather large amount (25%) of Sr ions does lower the superconducting transition temperature (to 70.5 K), although not as much as compared to that in samples doped with relatively much smaller amount of 3d elements. Doping with 3d elements strongly suppresses the area of the hysteresis of microwave absorption. Further, in the case of Mn-doped sample, the hysteresis is almost completely absent.

(ii) The Mn ions play a much more profound role in YBaCuO than in LaCuO ceramics. The samples $YBa_2Mn_{0.001}Cu_{2.999}O_{7-\delta}$, $YBa_2Mn_{0.005}Cu_{2.995}O_{7-\delta}$, and $YBa_2Mn_{0.01}Cu_{2.99}O_{7-\delta}$ which contain rather small amounts of Mn^{2+} ions exhibited significantly lower $T_c^{R=0}$. This is strongly in contrast to the superconducting samples $(La_{1-x}Ba_x)_2CuO_y$ doped with larger amounts of Mn (0.1 and 1.0 at.%), where Mn ions serve only as EPR probes, and do not alter $T_c^{R=0}$ [39].

(iii) In contrast to the pure sample, all the doped samples exhibit low-temperature anomalies in the ac-susceptibility, i.e. an increase of susceptibility with decreasing temperature in some ranges of temperature.

(iv) The value of the penetration depth (λ_0) increases significantly in the sample doped with Ni from that in the pure sample.

ACKNOWLEDGEMENTS

We acknowledge partial financial support from the Polish government (grant No. 2P302 060 04) and from National Sciences and Engineering Research Council of Canada (grant No. OGP0004485 — SKM). Thanks are due to Dr. J. L. Tholence (CRTBT, CNRS, Grenoble, France) for providing his apparatus for ac-susceptibility measurements.

REFERENCES

[1] Wu M. K., Ashburn J. R., Torng C. J., Hor P. H., Meng R. L., Gao L., Huang Z. J., Wang Y. Q., Chu C. W., *Phys. Rev. Lett.*, **58** (1987) 908.

[2] Ovshinsky S. R., Young R. T., Allred D. D., DeMaggio G., Van der Leeden G. A., *Phys. Rev. Lett.*, **58** (1987) 2579.

[3] Misra S. K., Misiak L. E., *J. Phys.: Condens. Matter*, **1** (1989) 9499.

[4] Misra S. K., Misiak L. E., *Solid St. Commun.*, **72** (1989) 1207.

[5] Ronay M., Newns D. N., *Phys. Rev.*, *B***39** (1989) 819.

[6] Mandal P., Poddar A., Choudhury P., Das A. N., Ghosh B., *J. Phys. C: Solid St. Phys.*, **20** (1987) L953.

[7] Vassilev P. G., *Physica*, *C***153–155** (1988) 868.

[8] Veit M., Langen J., Galffy M., Jostarndt H. D., Erle A., Blumenröder S., Schmidt H., Zirngiebl E., Güntherodt G., *Physica*, *C***153–155** (1988) 900.

[9] Bieg J., Jing J., Engelmann H., Hsia Y., Gnoser U., Gütlich P., Jakobi R., *Physica*, *C***153–155** (1988) 952.

[10] Moorjani K., Bohandy J., Kim B. F., Adrian F. J., Du Y. W., Tang H., Qiu Z. Q., Walker J. C., *J. Appl. Phys.*, **63** (1988) 4161.

[11] Pankhurst Q. A., Morrish A. H., Zhou X. Z., *Phys. Lett.*, *A***127** (1988) 231.

[12] Ishikava M., Takabatake T., Tohdake A., Nakazawa Y., Shibuya T., Koga K., *Physica*, *C***153–155** (1988) 890.

[13] Okuda K., Noguchi S., Maeno Y., Fujita T., *Physica*, *C***153–155** (1988) 880.

[14] Xiao G., Streitz F. H., Gavrin A., Cieplak M. Z., Chien C. L., Bakhshai A., *J. Appl. Phys.*, **63** (1988) 4196.

[15] Obradors X., Vallet M., Rodriguez J., Fontcuberta J., Labarta A., Gonzalez-Calbet J. M., *Physica*, *C***153–155** (1988) 888.

[16] Roth G., Heger G., Renker B., Pannetier J., Caignaert V., Hervieu M., Raveau B., *Physica*, *C***153–155** (1988) 972.

[17] Westerholt K., Arndt M., Wüller H. J., Bach H., Stauche P., *Physica*, *C***153–155** (1988) 862.

[18] Kuentzler R., Vilminot S., Dossmann Y., Derory A., *Physica*, *C***153–155** (1988) 1032.

[19] Adrian H., Bauer O., Niederhofer H., Adrian G., Nielsen S., *Physica*, *C***153–155** (1988) 928.

[20] Takano M., Hiroi Z., Mazaki H., Bando Y., Takeda Y., Kanno R., *Physica*, *C***153–155** (1988) 860.

[21] Greene L. H., Groud M., Bagley B. G., Tarascon J. M., Barbux P., Miceli P. F., Hull G. W., *Physica*, *C***153–155** (1988) 896.

[22] Liang R., Nakamura T., Kawaji H., Itoh M., Nakamura T., *Physica*, *C***170** (1990) 307.

[23] Cava R. J., Batlogg B., Chen C. H., Rietman E. A., Zahurak S. M., Werder D., *Phys. Rev.* *B***36** (1987) 5719.

[24] Vonsovsky S. V., Izyumov Yu. A., Kurmaev E. Z., *Superconductivity of Transition Metals*, Springer, Berlin 1982.

[25] Sung H. M., Kang J. H., Liang J. M., Liu R. S., Chen Y. C., Wu P. T., Chen L. J., *Physica*, *C***153–155** (1988) 866.

[26] Symko O. G., Zheng D. J., Durny R., Ducharme S., Taylor P. C., *Phys. Lett.*, *A*134 (1988) 72.
[27] Blazey K. W., Portis A. M., Bednorz J. G., *Solid St. Commun.*, **65** (1988) 1153.
[28] Misra S. K., Misiak L. E., *Solid St. Commun.*, **72** (1989) 117.
[29] Orlando T. P., McNiff E. J., Foner S., Beasly M. R., *Phys. Rev.*, *B*19 (1979) 4545.
[30] Korczak W., Korczak Z., Rysak A., *Proceedings of the RAMIS* 91 *Conference*, Poznań, Poland 1991.
[31] Mehran F., Barnes S. E., Tsuei C. C., McGuire T. R., *Phys. Rev.*, *B*36 (1987) 7266.
[32] Khoder A. F., Couach M., Monnier F., Henry J. Y., *Europhys. Lett.*, **15** (1991) 337.
[33] Orlando T. P., Delin K. A., Foner S., McNiff E. J., Jr., Tarascon J. M., Greene L. H., McKinnon W. R., Hull G. W., *Phys. Rev.*, *B*35 (1987) 7249.
[34] Okuda K., Noguchi S., Yamaguchi A., Sugiyama K., Date M., *Jpn. J. Appl. Phys.*, **26** (1987) L822.
[35] Pincus P., Gossard A. C., Jaccarino V., Vernick J. H., *Phys. Lett.*, **13** (1964) 21.
[36] Rakvin B., Pozek M., Dulcic A., *Solid St. Commun.*, **72** (1989) 199.
[37] Harshman D. R., Aeppli G., Ausaldo E. J., Batlogg B., Brewer J. H., Carolan J. F., Cava R. J., Celio M., Chaklader A. C. D., Hardy W. N., Kreitzman S. R., Luke G. M., Noakes D. R., Senba M., *Phys. Rev.*, *B*36 (1987) 2386.
[38] Niki H., Suzuki T., Tomiyoshi S., Hentona H., Omori M., Kajitani T., Kamiyama T., Igei R., *Solid St. Commun.*, **69** (1989) 547.
[39] Kikuchi H., Ajiro Y., *J. Phys. Soc. Jpn.*, **57** (1988) 2628.

STRESZCZENIE

Opór, zmiennoprądowa podatność magnetyczna i niskopolowa absorpcja mikrofalowa (pasmo X) w próbkach wysokotemperaturowego nadprzewodnika $YBa_2Cu_3O_{7-\delta}$ domieszkowego Gd, Sr, Cr, Mn, Fe i Ni zostały zmierzone w zakresie temperatur 4,2–295 K w celu zbadania efektu niskiego poziomu domieszkowania na własności nadprzewodzące badanych próbek. Wartości górnych pól krytycznych, stałych Sommerfelda i temperatur przejścia były wyznaczone z danych absorpcji mikrofalowej. Stwierdzono, że obecność nawet małych ilości pierwiastków 3d ma znaczny wpływ na własności nadprzewodzące wysokotemperaturowych nadprzewodników $YBa_2M_xCu_{3-x}O_{7-\delta}$.